

## The Impact of Cationic Surfactants on The Electrodeposition of Nickel/Graphene Nano-Sheet Composite Coatings on Brass

M.A.Ameer<sup>1</sup>, Z. Abdel Hamid<sup>2</sup>, M. Shehata<sup>1\*</sup>, B.M. Hassan<sup>1</sup>, A.M. Fekry<sup>1</sup>

<sup>1</sup>Chemistry Department, Faculty of Science, Cairo University, Giza -12613, Egypt.

<sup>2</sup>Corrosion Control and Surface Protection Department, CMRDI, Helwan, Cairo, Egypt.

GRAPHENE nano-sheets (GNS) and cationic surfactants (S1&S2) are utilized for nickel composite coatings electrodeposition. They have a significant role in increasing the corrosion resistance of these coatings. A use of Nickel watt's bath with the addition of GNS as reinforcement material and different surfactants for nano-composite coatings deposition (Ni-GNS) are considered and the outcomes have been examined and discovered. Electrochemical techniques are utilized for examining the corrosion resistance for samples of nano-composite coatings in 0.6 M NaCl. The results suggest that the content of incorporated GNS increases with increasing the extent of GNS in plating bath. All of the Ni-GNS nano-composite layers in presence of surfactant have better corrosion resistance than the nickel coating. The best corrosion resistance value of about 64 kΩ cm<sup>2</sup> and relatively highest hardness value of 509 Hv for the composite coating electrode of Ni-GNS/with S1 are in comparison with the rest of nano-composite coating electrodes or pure Ni coatings.

**Keywords:** Electrodeposition, Ni-GNS nanocomposite coating, Reinforcement, Corrosion resistance, Surfactant, Electrochemical techniques.

### Introduction

Deposited Ni are utilized expansively in numerous requests such as aerospace, automotive industry for steel plating, marine, mining, agriculture, nuclear fields, dyes, in the creation of musical instruments and small aircraft microelectronics. It is also utilized in micro electromechanical systems, precision engineering, medical device due to high corrosion resistance and mechanical properties [1]. The coatings formed by electroplating have characteristics generally based on the bath chemical components, temperature, applied current, additives, reinforcement and pH value [2]. Moreover, high ionic conductivity of electrolyte in electroplating bath makes particles tend to get agglomerated [3]. Ni coatings can enhance the amount and the distribution of co-deposited particles by adding organic materials like surfactants and inert ceramic particles (reinforcement) in an electrolytic bath [4-6]. The reinforcement in the Ni plating bath makes recrystallization of the metals [7]. GNS is a material that can be utilized in numerous disciplines including: bioengineering, composite materials, energy technology and nanotechnology. It is a two-dimensional nano-sheet of carbon

atoms which have extra attention and it has been applied into sensors, electrodes, solar cells and fuel cells [8] due to its high mechanical strength, high specific surface area, excellent clearness, and high conductivity. In addition, GNS can work as an oxidation barrier even at high temperature because it has an inert and impervious character and also it can significantly improve the corrosion resistance of substrates [9, 10]. Electrodeposition of Ni-GNS-TiO<sub>2</sub> nano-composite coating has been studied by Z. Abdel Hamid et al [11]. In a recent investigation, graphene is used as reinforcement for Ni electrodeposition composite coatings with high amount of GNS, good dispersion and high hardness was observed [12]. The surface morphology of the composite coating improved due to the incorporation of nanometer GNS [13]. Nano-sheets prevent disturbance actions and recrystallization processes at elevated temperatures increasing microhardness and thermal constancy [14]. Many researchers investigated different types of surfactants and its concentrations on the codeposition process [15-20].

This work has been made to investigate the influence of the concentration of two new cationic

\*Corresponding author e-mail: mohammed.shehata9011@yahoo.com; Tel: 202 01011551545

DOI: 10.21608/ejchem.2018.4598.1404

©2017 National Information and Documentation Center (NIDOC)

surfactants (S1&S2) on the amount of GNS co-deposited with Ni on brass substrate and its corrosion resistance in 0.6M NaCl electrolyte.

## Experimental

### Chemicals and material

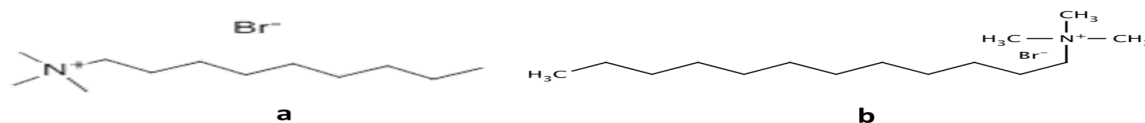
Natural graphite fine powder extra pure with particle size <50  $\mu\text{m}$  (merck) was utilized to synthesize GNS. Pure ammonia solution (33% Fluka) was utilized for pH modification.  $\text{H}_2\text{SO}_4$  (95–97%),  $\text{NaNO}_3$  (from -Sigma-Aldrich-),  $\text{H}_2\text{O}_2$  (30%-Alpha Chemika) and  $\text{KMnO}_4$  analytical grade were utilized.

### Preparation of GNS.

Hummers' method as reported in literature [21, 22] was used for preparing GNS.

### Electrodeposition process

Pure Ni and Ni-GNS coats were deposited on brass sheet; each has dimensions of 64 mm  $\times$  40 mm  $\times$  0.4 mm using Ni-watt's bath solution. The chemical confirmation of brass is (%): 60.66 Cu, 36.58 Zn, 1.02 Pb and %1.74 Fe. The composition of Ni-watt's bath is ( $\text{gL}^{-1}$ ) [23]: 300  $\text{NiSO}_4$ , 60  $\text{NiCl}_2$ , 45  $\text{H}_3\text{BO}_3$  at 50°C and at pH= 4.5. Pure Ni metal is denoted as the anode and brass slides were utilized as cathode. After electroplating process brass surface must be treated from oils, greases and rust: polished brass surface using different grade of emery papers to get refined and lustrous surface, then degreased by dipping in an alkaline solution ( $\text{NaOH}$ ,  $\text{Na}_3\text{PO}_4$  and  $\text{Na}_2\text{CO}_3$ ) at 70 °C, and it was rinsed with distilled water. Then it was dropped in 10% HCl to remove the residual (pickling). After that it was washed with distilling water and dried. Finally, the electrode was ready to electroplating process. The pH value of electrolyte adapted 4.5 by using ammonia solution and/or 10%  $\text{H}_2\text{SO}_4$ . Different operating conditions were tested to prepare the specimens. The electrodeposition process was operated at different current densities (c.d.) from 20 to 40  $\text{mAcm}^{-2}$  and different concentrations of GNS (0–0.3  $\text{gL}^{-1}$ ). Different concentrations for two types of cationic surfactants were used: Nonyltrimethyl ammonium bromide, S1 (Scheme 1 a) and Dodecyl trimethyl ammonium bromide, S2 (Scheme 1 b)



**Scheme 1.** Molecular structure of a) Nonyltrimethyl ammonium bromide (S1) and b) Dodecyl trimethyl ammonium bromide (S2).

*Egypt. J. Chem.* **62**, No. 2 (2019)

### Thickness measurement.

The thickness Gauges are used to measure the coating layer thickness (Qnix® 8500, automation Dr.nix, GmbH, Germany). The thickness was measured at several places on the specimen and the average value was obtained.

### Electrochemical measurements

The electrochemical characteristics are investigated by two different techniques: potentiodynamic polarization Tafel lines and EIS in 0.6 M NaCl electrolyte. All electrochemical measurements were investigated using electrochemical EC-Lab Bio-Logic SAS, Software Version 10.38, Model: VMP3. A typical three-electrode glass cell was used. The working electrodes were brass, electrodeposited Ni/brass, Ni-GNS/brass and Ni-GNS with S1&S2/brass, surface area exposed to electrolyte solution was 2.0  $\text{cm}^2$ . The reference electrode was  $\text{Hg}/\text{Hg}_2\text{Cl}_2/\text{Cl}^-$  (SCE) and the auxiliary electrode was a platinum slide. 0.6M NaCl solution prepared using triply distilled water. Polarization tests were performed after reaching  $E_{\text{corr}}$  and EIS measurements were done in the frequency range of 100 kHz–100 mHz with an amplitude of 10 mV at the open circuit potential. The electrode potential was endorsed to become stable for 30 min before measurements. All experimentations were supported at room temperature in air.

### Surface characterization using (SEM-EDX) system.

Scanning electron microscopy (SEM, JEOL—JSM 6060 LV) was used to observe the surface morphology of the deposits. Moreover the elemental analysis of the deposited layer was studied using Energy dispersive X-ray system (EDX) model JEOL, JSM-5410.

### Mechanical properties.

As stated in reference [24].

Adhesion properties of the codeposited coatings were carried out using the cross-cut method (scratch test method) and classification according to ISO specification 2409.

## Results and Discussion

### Effect of current density (c.d.)

Current density is the main parameter controlling the deposition rate which in turn affect the composition and the morphology of the coating layer and the concentration of integrated reinforcement of the coatings. It also influences the thickness of the composite film, in the way that, as the c.d. increases, the thickness of the coatings increases as well reaching an optimum value. Electrodeposition process consists of nucleation, growth mechanisms and thickening of the primary layer. The nucleation boosted by high c.d. contrastive from the growth process [25].

The data of c.d. effect tabulated in Table 1a, which lists the thickness of pure Ni coatings deposited at different c.d. (20, 30 and 40 mAcm<sup>2</sup>) on brass substrates and standard deviation ( $\sigma$ ) values for five measured values in several places for each sample. The highest thickness (14.2  $\mu$ m) is at c.d.30 mAcm<sup>2</sup>.

Potentiodynamic polarization measurements were achieved in the range from -1.30 V to -0.35 V vs. SCE, at a scan rate of 1.0 mV s<sup>-1</sup> in 0.6M NaCl, where the corrosion rate (C.R.) is proportional to the corrosion current density. Polarization parameters ( $i_{\text{corr}}$ ,  $E_{\text{corr}}$ ,  $\beta_a$  and  $\beta_c$ ) are given in Table 2(a&b) and measured as reported in our previous work [26]. C.R. is calculated from:  $\text{C.R.} = (i_{\text{corr}} \cdot K)$ .

**TABLE 1. The thickness of Ni, Ni-GNS, Ni-GNS/ with S1 and with S2 nanocomposite coatings (prepared at different concentrations of GNS, S1 and S2 in the Ni watt's bath which the standard deviation ( $\sigma$ ) values for the five measured values in different places for each sample and EDX analysis data at different c.d. on brass.**

	Parameter Effect	Thickness ( $\mu$ m)	Standard deviation		Wt%	
			( $\sigma$ )		C	Ni
	c.d (mAcm <sup>2</sup> )					
A	20	13.1	0.498			100
	30	14.2	0.880			100
	40	11.4	0.975			100
	GNS (gL <sup>-1</sup> )					100
B	0.1	11.6	0.989		3.98	96.02
	0.2	14.6	0.747		10.40	89.60
	0.3	13.2	0.543		5.73	94.27
	S1 (ppm)					
C	300	12.5	0.408		16.82	83.18
	400	16.2	0.886		19.38	78.35
	500	16.9	0.464		19.06	80.94
	S2 (ppm)					
D	200	12.6	0.270		14.95	85.05
	300	14.3	0.480		21.65	80.62
	400	13.7	0.680		16.82	83.18

EW)/d.A, Where  $i_{\text{corr}}$  is the corrosion current (in ampere), K a constant that defines the units of the C.R (3272 mm/ A cm y), EW the equivalent weight (in g/equivalent), d the density (in gcm<sup>-3</sup>) and A the sample area (in cm<sup>2</sup>). The C.R. value for the tested coated alloy has minimum value (0.00323 mmy<sup>-1</sup>) at 30 mA cm<sup>-2</sup> and at the same c.d, C.R. increases with immersion time from 1hr to 672hrs (Table 2 a&b, Fig. 1 a&c). So, 1h immersion is preferred.

Figure 2 (a- c) represents Bode, phase angle and Nyquist (in situ) plots of Ni coatings at 30 mA cm<sup>-2</sup> on brass substrate with different immersion times (1hr, 336hrs and 672hrs) in 0.6 M NaCl. The semicircle depresses highly with increasing time denoting a high resistance at 1 hour. The best model fits the experimental data (Fig. 3) is two time constants:  $R_s$  is the solution resistance,  $Q_{\text{out}}$  and  $R_{\text{out}}$  are the impedance response to capacitance and resistance due to the coating, and finally  $Q_{\text{inn}}$  and  $R_{\text{inn}}$  are capacitance of the double layer and resistance to the charger transfer. A constant-phase element (CPE) is utilized in place of the ideal capacitance to explain the non-smooth surface [27]. The impedance of CPE is  $Z_{\text{CPE}} = [C(j\omega)^n]^{-1}$ , where  $-1 \leq n \leq 1$ . The value of n is due to non-smooth surface. From the data (Table 3 a-c), it is clear that at different c.d., the best total resistance,  $R_{\text{out}} + R_{\text{inn}}$  ( $R_t$ ), values for Ni coated on brass without GNS is at c.d. 30 mA cm<sup>-2</sup> as achieved by all other utilized techniques through this work.

The next sessions illuminate the effect of different operating conditions on the nano-composite coating products at  $30 \text{ mA cm}^{-2}$ .

#### Effect of graphene concentration (GNS)

The surface morphology for pure nickel slide without any modification was imaged using SEM microscopic analysis at Fig. 4 a. The effect of adding different concentrations of GNS at  $30 \text{ mA cm}^{-2}$  have been investigated through SEM analysis (See supplementary data Fig. 1 a-c). As well thickness measurements and EDX analysis data at different GNS concentrations ( $0.1\text{-}0.3 \text{ gL}^{-1}$ ) (Table 1 b & Fig. 4 b) can reveal that the optimum concentration of GNS is  $0.2 \text{ gL}^{-1}$  at  $30 \text{ mA cm}^{-2}$  which can also be confirmed by EDX image (See supplementary data Fig. 1 d).

EIS tests are performed in  $0.6\text{M}$  NaCl solution to

study the anti-corrosion properties of the composite coatings obtained at different immersion times [12,28].

Figure 2 a-c. exemplified the Bode, phase angle and Nyquist (in situ) plots of substrate and composite coatings prepared at  $30 \text{ mA cm}^{-2}$  without and with  $0.2 \text{ g L}^{-1}$  at different immersion times. It proved that the pure Ni coatings exhibited poor corrosion resistance property than Ni-GNS coating. Moreover, the coating deposited at  $0.2 \text{ gL}^{-1}$  GNS have higher impedance than the coating deposited in nonexistence of GNS. Meanwhile, the obtained EIS spectra of coatings deposited in absence of GNS showed narrow semicircles. In fact, the diameter of the semicircles decides the anti-corrosion property of coatings and the larger diameter ensures the better corrosion resistance [12].

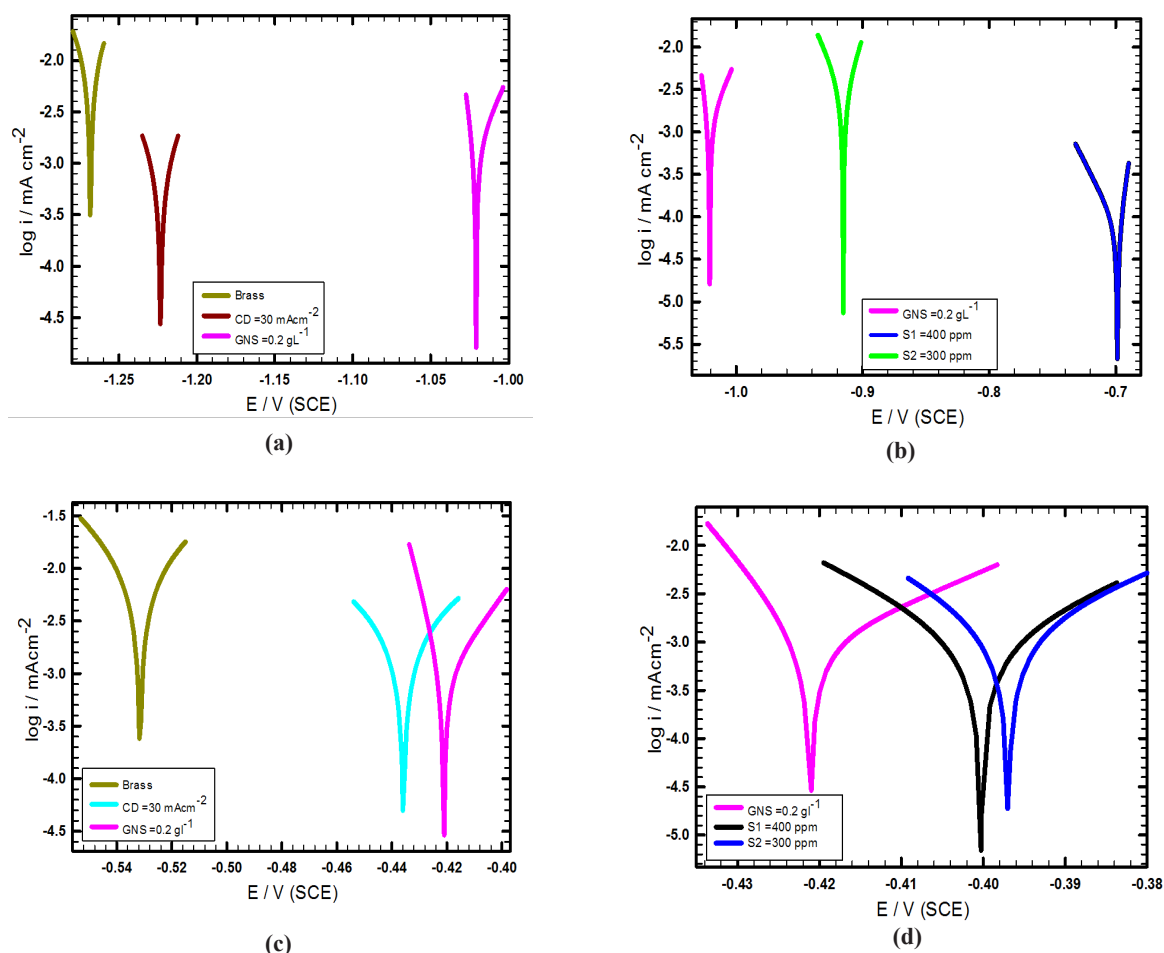


**Fig.1 (a-d).** Polarization scans of a) brass, Ni coats at c.d  $30 \text{ mA cm}^{-2}$  on brass and in presence of  $0.2 \text{ g L}^{-1}$  GNS after 1hr. b)  $0.2 \text{ g L}^{-1}$  GNS, S1 400 ppm and S2 300 ppm after 1hr, c) brass, Ni coats at c.d  $30 \text{ mA cm}^{-2}$  on brass and in presence of  $0.2 \text{ g L}^{-1}$  GNS after 672 hrs. d)  $0.2 \text{ g L}^{-1}$  GNS, S1 400 ppm and S2 300 ppm after 672hrs in  $0.6 \text{ M}$  NaCl.

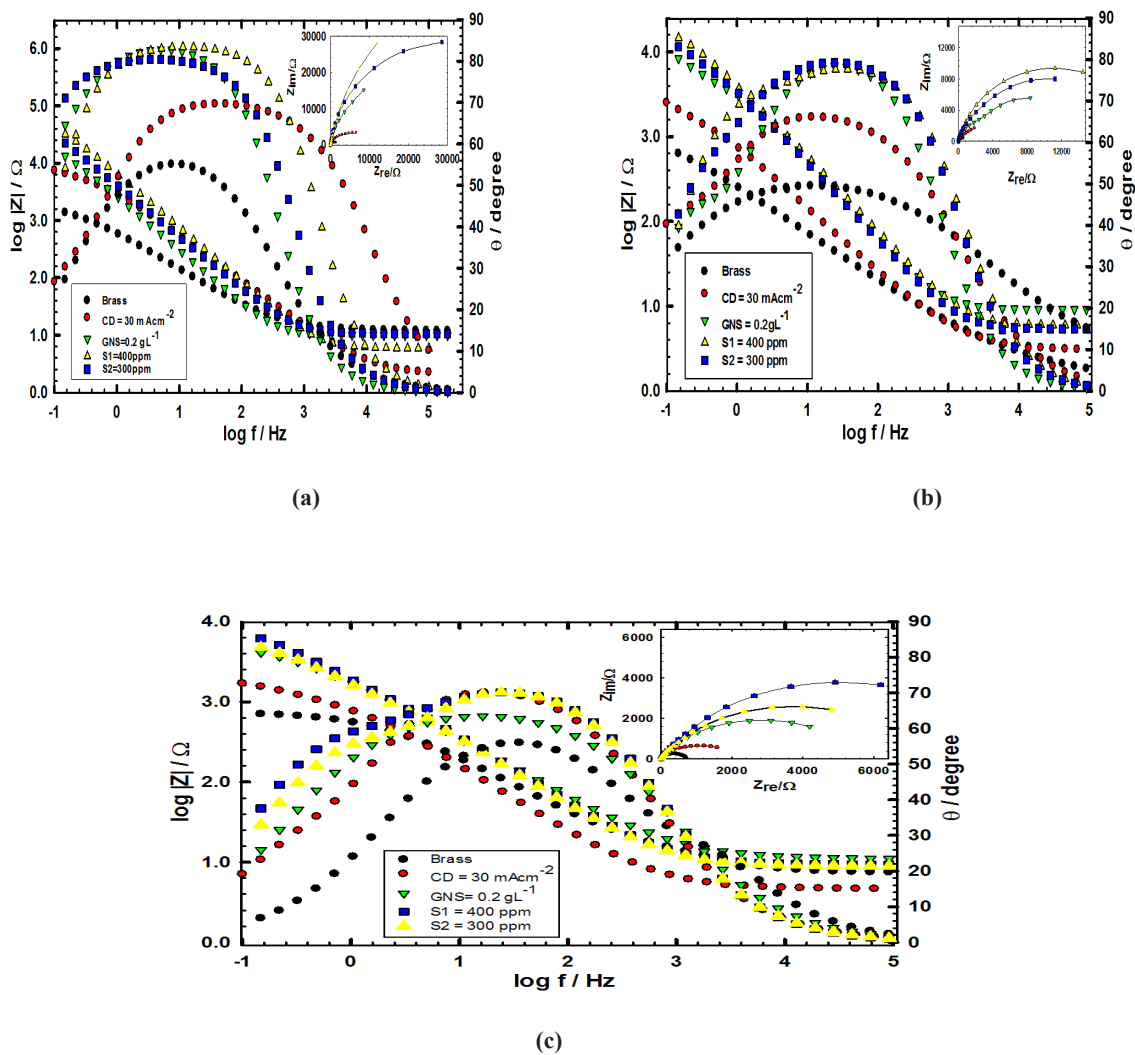


Fig. 2 (a-c). Bode, phase angle and Nyquist (in situ) plots of Ni coats at  $30\text{mAcm}^{-2}$  on brass in presence of  $0.2\text{gL}^{-1}$  GNS, 400 ppm S1 or 300 ppm S2 in  $0.6\text{M NaCl}$ : a) after 1hr, b) after 336 hrs and c) after 672 hrs.

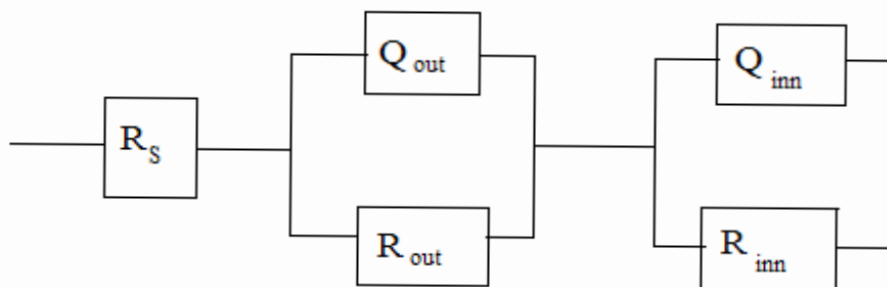
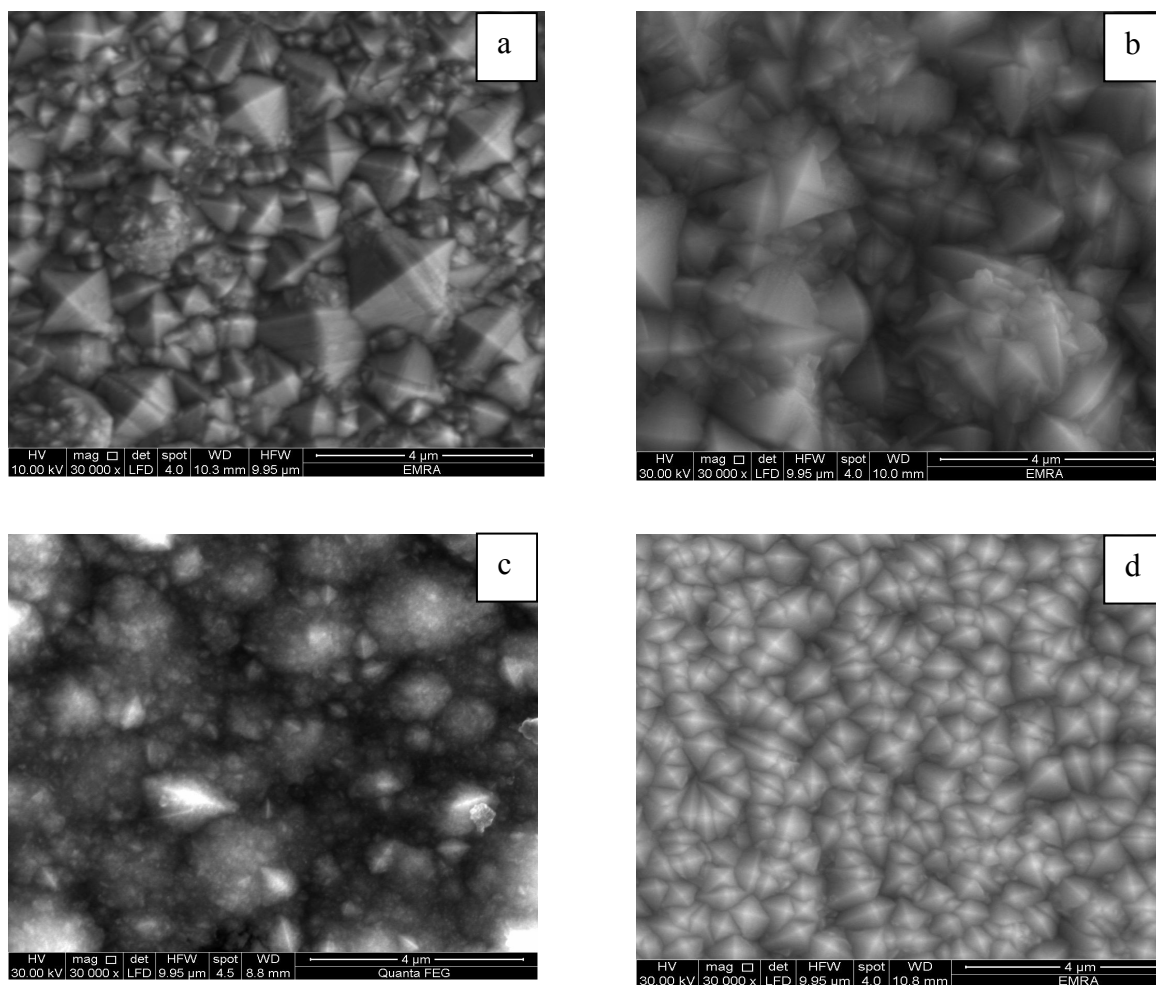


Fig. 3. Equivalent circuit model representing two time constants for an electrode / electrolyte solution interface.



**Fig.4 (a-c).** SEM images of brass coated with: a) Ni, b) Ni-GNS c) Ni-GNS/ with S1 and d) Ni-GNS/ with S2 nanocomposite.

Potentiodynamic polarization data (Table 2 a&b, Fig. 1 a&c) confirms the results of EIS (Table 4 a-c). Addition of  $0.2 \text{ gL}^{-1}$  GNS decreases C.R. from 0.00323 to 0.00216 after 1hr and increases it slightly to  $0.0037 \text{ mm.y}^{-1}$  after 672 hrs. Figure 5 denotes a decrease of C.R. and an increase of  $R_p$  on different immersion times which also can be explained by a reduction of metallic surface that can be accessed to the corrosive ambience [29].  $R_p$  increase from  $12.005 \text{ K}\Omega \text{ cm}^2$  (in nonexistence of GNS) to  $66.270 \text{ K}\Omega \text{ cm}^2$  (in existence of  $0.2 \text{ gL}^{-1}$  GNS) at  $30 \text{ mA cm}^{-2}$  after 1hr immersion. After 672 hrs,  $R_p$  decreases (Table 4 a-c).

The factors responsible for improving C.R. may be the uniformly distribution of GNS lamina which fills the micro punctures and incisions in the Ni matrix, homogeneous dispersion of GNS during the deposition process and inert physical hindrance feature of GNS are responsible for improved C.R. [12, 28].

*Egypt. J. Chem.* **62**, No. 2 (2019)

#### *Effect of surfactants*

Two different surfactants are used to improve the deposition and coating properties: Nonyltrimethyl ammonium bromide, S1 (Scheme 1 a) and Dodecyl trimethyl ammonium bromide, S2 (Scheme 1 b).

The thickness data tabulated in Table 1 (c&d) in order to show the thickness of deposited Ni coats at optimum conditions ( $30 \text{ mA cm}^{-2}$  and GNS concentration of  $0.2 \text{ gL}^{-1}$ ) on brass. It is clear that the highest thickness ( $16.2 \mu\text{m}$ ) is obtained at S1 concentration = 400 ppm and ( $14.3 \mu\text{m}$ ) for S2 concentration = 300 ppm.

SEM as well as EDX analysis performed to study the effect of adding different concentrations of both surfactants (S1&S2). For S1 Fig. 2 (a-c) (See supplementary data) we can see the change of the morphology for each slide on adding different concentrations of S1. These additions make

enhancement for the amount of deposit GNS on the surface at optimum concentration of S1= 400 ppm (Fig. 4 c) and (Fig. 2 d at supplementary data)

In the same way, for S2 (Fig. 3 a-c) (See supplementary data) we can also notice a similar change for each slide on adding different concentrations of S2. From these analyses, the optimum concentration for S2 could be found at 300 ppm (Fig. 4 d) and (Fig. 3 d at supplementary data)

The polarization results (Table 2 a&b) reveal that, adding different concentrations of S1 (300, 400 and 500 ppm) in existence of 0.2 gL<sup>-1</sup> GNS at 30 mA cm<sup>-2</sup> increase the R<sub>T</sub> and decrease C.R. of the coating layer in 0.6M NaCl. The optimum concentration of S1 is 400 ppm which corresponding to maximum R<sub>T</sub> and minimum C.R (Fig. 1 b&d).

Moreover, in case of using S2 (200, 300 and 400 ppm), the optimum concentration is 300 ppm which corresponding to maximum R<sub>T</sub> and minimum C.R. Comparing to the data of S1 and S2, it is clear from EDX analysis data (Table 1 c&d) that, the wt% of GNS is maximum for S1 at 400 ppm and for S2 at 300 ppm.

Figure 2 a-c. represents the Bode, phase angle and Nyquist (in situ) plots of substrate and composite coatings prepare at 30 mA cm<sup>-2</sup> and with 0.2gL<sup>-1</sup> at different immersion times. It proves that the Ni-GNS coat exhibit poor corrosion resistance property than Ni-GNS/ with S1&S2 coats. Moreover, the coating deposit at 400 ppm S1 has higher impedance than coating deposit in absence of S1. Meanwhile, the obtained EIS spectra of coats deposit in absence of GNS show narrow semicircles. Table 4 a-c data confirm the results of polarization results (Table 2 a&b).

**TABLE 2. Electrochemical parameters derived from Tafel lines at different immersion time for electrodeposited Ni/brass, Ni-GNS/brass and Ni-GNS-with Surfactant/brass at different concentration of GNS, S1 and S2 nanocomposites deposited at 30 mAcm<sup>-2</sup> in 0.6 M NaCl at 25 °C. a) After 1hr b) after 672 hrs.**

Time (hrs)	condition	E <sub>corr</sub> V (SCE)	I <sub>corr</sub> μA cm <sup>-2</sup>	β <sub>a</sub> mV dec <sup>-1</sup>	-β <sub>c</sub> mV dec <sup>-1</sup>	C.R., mmy <sup>-1</sup>	P.E %
a) 1							
	Brass	-1.268	3.40	42.8	33.7	0.02440	-
	CD=30mAcm <sup>-2</sup>	-1.223	0.60	36.4	37.2	0.00323	82.35
	GNS=0.1gL <sup>-1</sup>	-1.145	0.93	15.6	16.6	0.00503	72.56
	GNS=0.2gL <sup>-1</sup>	-1.022	0.40	19.0	29.8	0.00216	88.24
	GNS=0.3gL <sup>-1</sup>	-1.152	0.88	46.5	51.5	0.00474	74.12
	S <sub>1</sub> =300ppm	-0.815	1.15	34.1	21.3	0.00620	66.17
	S <sub>1</sub> =400ppm	-0.701	0.036	17.2	21.7	0.00020	98.92
	S <sub>1</sub> =500ppm	-1.013	0.98	23.7	25.8	0.00530	71.17
	S <sub>2</sub> =200ppm	-1.006	1.13	30.0	31.5	0.00607	66.88
	S <sub>2</sub> =300ppm	-0.915	0.013	33.0	25.5	0.00007	99.61
	S <sub>2</sub> =400ppm	-1.037	1.26	38.7	24.9	0.00680	62.94
b) 672							
	Brass	-0.532	7.5	23.4	25.4	0.0400	-
	CD=30mAcm <sup>-2</sup>	-0.436	0.8	90.4	96.9	0.0043	89.34
	GNS=0.1gL <sup>-1</sup>	-0.441	1.5	79.4	75.9	0.00810	80.00
	GNS=0.2gL <sup>-1</sup>	-0.421	0.7	43.0	37.5	0.00370	90.40
	GNS=0.3gL <sup>-1</sup>	-0.478	1.7	48.3	64.5	0.00916	77.34
	S <sub>1</sub> =300ppm	-0.412	1.3	90.3	80.9	0.0070	82.67
	S <sub>1</sub> =400ppm	-0.401	0.336	23.9	27.6	0.00181	95.52
	S <sub>1</sub> =500ppm	-0.455	1.45	19.7	20.7	0.0078	80.67
	S <sub>2</sub> =200ppm	-0.472	1.25	36.3	31.8	0.00674	83.34
	S <sub>2</sub> =300ppm	-0.397	0.425	22.1	29.4	0.00230	94.34
	S <sub>2</sub> =400ppm	-0.411	1.94	18.9	23.2	0.01000	74.13

**TABLE 3. Electrochemical parameters derived from EIS for different current density (containing different concentrations of GNS nanocomposite and without GNS) in 0.6M NaCl at 25 °C. a) after 1 hr b) after 336 hrs c) after 672 hrs.**

Time (hrs)	condition	Rs $\Omega \text{ cm}^2$	Rout $\Omega \text{ cm}^2$	Qout $\mu\text{F cm}^{-2}$	Rinn $\Omega \text{ cm}^2$	Qinn $\mu\text{F cm}^{-2}$	n	P.E %
a)1	Without GNS							
	20	7.75	2522.7	277.2	7316	104.5	0.97	77.11
	30	8.75	3027.0	292.8	8978	94.03	0.99	81.24
	40	6.49	1869.0	363.7	5884	153.7	0.97	70.9
	With GNS							
	20	10.92	5451.0	271.87	31646	180	0.95	93.9
	30	11.91	8471.0	136.2	57799	134	0.97	96.6
	40	10	2699.0	226.2	26082	170	0.99	92.1
b)336	Without GNS							
	20	3.75	611.10	427	495	253.61	0.95	33.38
	30	6.16	1463.0	329.5	6401	125	0.96	78.88
	40	5.18	1024.4	366.7	707.8	193.2	0.99	43.2
	With GNS							
	20	9.22	2403.0	231.34	18260	205	0.97	91.96
	30	10.7	3780.0	193.1	19675	153	0.95	92.92
	40	9.13	1044.0	262.35	6602	212	0.94	78.28
c)672	Without GNS							
	20	2.56	330.60	670.9	1238	312.72	0.97	48.61
	30	3.24	832.20	494.4	1702	224.53	0.98	68.19
	40	2.3	295.60	585.03	922.3	352.37	0.95	33.8
	With GNS							
	20	8.3	743.00	306.69	3857	272.24	0.95	82.5
	30	8.47	1356.0	242	5660	209.8	0.98	88.5
	40	7.244	523.00	390.29	1571	310.29	0.99	61.5

Zeta potential is acute for avoiding collection and hanging nanoparticles into the electrolytes as informed by others [30]. For GNS of  $-ve$  zeta potential, adding cationic surfactant results in increasing surface  $+ve$  charge with increasing its concentration, preventing sheets agglomeration and decrease sedimentation.

As demonstrated in Fig. 5, the absolute zeta potential of GNS becomes of higher  $-ve$  charge, increasing the repulsive electrostatic force amongst the sheets. So, the extent of GNS increases and extra molecules will act as an electrolyte, increasing the ionic strength of the bath [15], constructing smaller multilayer, decreasing electrostatic repulsion and increasing agglomeration. Figure 5 exemplifies zeta potential measurements vs. pH, increasing  $-ve$  charge of zeta potential leads to suspending more GNS into the electrolyte and more co-deposition on the plated layer. Zeta potential has a higher negative value of  $-13.0$  mV at pH 4, thus

negative potential value helps in adsorption of surfactants on the Ni-GNS nanocomposite. Due to the existence of mechanical agitation, transport of the GNS to the cathode surface occurs by the fluids flux to the cathode. Then, they will hold on the cathode surface by the extrinsic force and be included by the deposited metal [31].

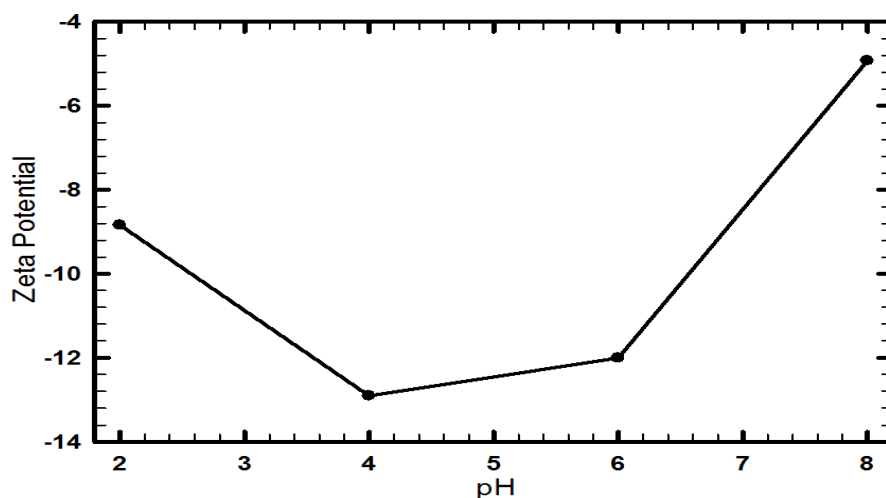
Therefore, using of surfactants in plating is improving the efficiency of codeposition process of Ni-GNS nanocomposite coatings.

Table 5 tabulates the data of mechanical properties hardness of Ni/ brass and Ni-GNS/brass in existence and nonexistence of surfactants at  $30 \text{ mAcm}^{-2}$ . The maximum hardness (509 Hv) is consistent with the optimum concentration of S1. This also, resulted by increasing content of reinforce nanosheet in the coatings. The minimum hardness of coatings was relevant to the specimen in absence of GNS and surfactants (225 Hv). It reveals that GNS have an effective



**TABLE 4.** Electrochemical parameters derived from EIS for Ni-GNS/brass, Ni-GNS-S1/brass and Ni-GNS-S2/Brass deposited at 30 mA cm<sup>-2</sup> in 0.6 M NaCl at 25 °C. a) after 1 hr b) after 336 hrs c) after 672 hrs.

Time (hrs)	condition	R <sub>s</sub>	R <sub>out</sub>	Q <sub>out</sub>	R <sub>inn</sub>	Q <sub>inn</sub>	n	P.E
		Ω cm <sup>2</sup>	Ω cm <sup>2</sup>	μFcm <sup>-2</sup>	Ω cm <sup>2</sup>	μFcm <sup>-2</sup>		%
a) 1	GNS= 0.1gL <sup>-1</sup>	8.71	4438	139.4	8934	136.4	0.99	83.16
	GNS=0.2gL <sup>-1</sup>	11.44	8471	136.2	57799	125.8	0.97	96.6
	GNS=0.3gL <sup>-1</sup>	10.7	6507	152.7	32085	134.5	0.94	94.16
	S1=300 ppm	8.62	3905	119.57	29395	103	0.98	93.24
	S1=400 ppm	9.318	6940	75	63692	28.66	0.97	96.8
	S1=500 ppm	9.181	5377	82.54	34354	56.9	0.99	94.33
	S2=200 ppm	9.935	934	57.3	37174	44.64	0.99	94.1
	S2=300 ppm	10.01	1549	45.94	122429	40	0.97	98.18
	S2=400 ppm	9.1	839	55.55	38225	43.1	0.94	94.23
b) 336	GNS=0.1gL <sup>-1</sup>	8.33	1382	394	2943	187.46	0.98	61.6
	GNS=0.2gL <sup>-1</sup>	10.05	2933	242	11325	154.34	0.99	88.35
	GNS=0.3gL <sup>-1</sup>	8.11	1291	489	2881	256.27	0.98	60.2
	S1=300 ppm	6.858	1206	286	5002	200	0.98	73.25
	S1=400 ppm	8.304	3805	189	20282	148.13	0.97	93.1
	S1=500 ppm	7.951	1764	270.96	6919	236	0.99	80.87
	S2=200 ppm	7.785	637	148.08	6241	103	0.97	75.85
	S2=300 ppm	8.857	928	107	17558	82.57	0.95	91.01
	S2=400 ppm	4.935	469	179.31	3076	130.2	0.94	53.16
c) 672	GNS=0.1gL <sup>-1</sup>	7.35	645	500	4800	400	0.95	85.2
	GNS=0.2gL <sup>-1</sup>	7.58	1467	350	5660	300	0.94	88.69
	GNS=0.3gL <sup>-1</sup>	6.98	568	520	2155	370	0.97	70.39
	S1=300 ppm	4.62	499.51	352	4600	246	0.95	84.19
	S1=400 ppm	5.911	1473.1	213	9340	190	0.94	92.54
	S1=500 ppm	5.263	510.1	340.9	4701	235	0.96	84.53
	S2=200ppm	4.231	314	250	1713	187.06	0.97	60.58
	S2=300ppm	5.074	489.1	186	7079	171	0.95	89.35
	S2=400ppm	3.98	213.7	233.3	1541	164	0.98	54.06

**Fig. 5.** Zeta potential measurement of GNS composite vs pH.



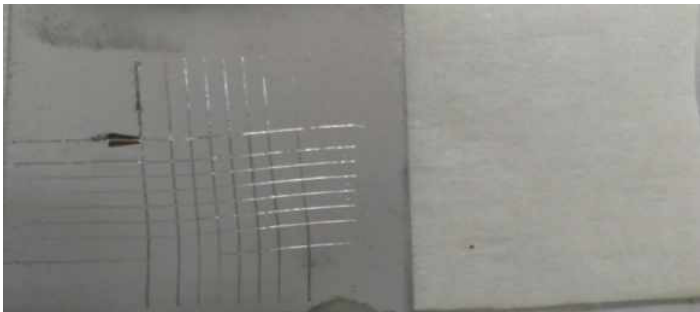
**TABLE 5. Mechanical properties hardness Ni/brass and Ni-GNS/brass in absence and presence of surfactants at 30mA cm<sup>-2</sup>.**

Samples	wt.% of GNS in coating layer	Hardness (HV)
Ni/brass	–	225
Ni-GNS/brass	10.4	315
Ni-GNS-S1/brass	19.38	509
Ni-GNS-S2/brass	21.65	495

role in mechanical properties promotes the microhardness. In fact, the utilized surfactants are the basis to absorb more GNS into the Ni matrix, and this phenomenon led to an increase of Nano hardness. It should be mentioned that GNS deposited into Ni matrix plays the role of obstacles versus the growth of the Ni grains and the plastic deformation of the matrix {Lee, 2007 #27; Lee, 2007 #29}.

The adhesion performance of the investigated samples can be evaluated using scratch testing. Table 6 data refers to the appropriate standard ISO 2409. Most of the samples have the edges of the cuts are completely smooth none of the squares of the lattice is detached (class zero). While, some detachment of flakes of the coating at the intersections of the cuts are not completely smooth and referring to ISO 2409 a cross cut is not significantly greater than 5 % is attached (class one).

**TABLE 6. The adhesion performance of the investigated samples was evaluated using scratch testing according to the appropriate standard ISO 2409.**

Sample condition	Image after scratching	Class according ISO
Pure Ni at different current density c.d =20 mAcm <sup>-2</sup>		Zero
c.d =30 mAcm <sup>-2</sup>		Zero
c.d =40 mAcm <sup>-2</sup>		One

At constant  
c.d 30 mA  
cm<sup>-2</sup>  
and different  
concentration  
of GNS  
GNS =0.1  
gL<sup>-1</sup>



**Zero**

GNS =0.2  
gL<sup>-1</sup>



**Zero**

GNS =0.3  
gL<sup>-1</sup>



**One**

At constant  
c.d =30 mA  
cm<sup>-2</sup> and GNS  
=0.2 gL<sup>-1</sup>  
S1 =300 ppm



**Zero**

S1 =400 ppm

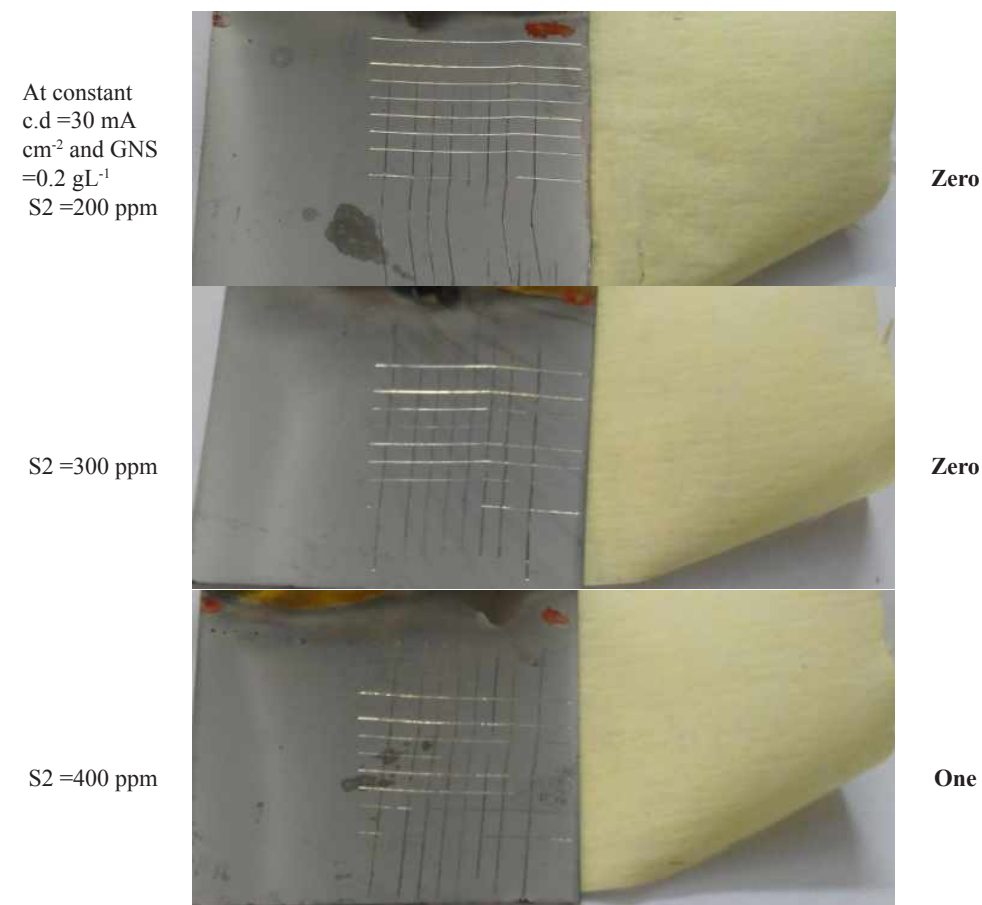


**Zero**

S1 =500 ppm



**One**



### Conclusion

In this paper, Ni-GNS nano composite coatings were efficaciously electrodeposited at 50°C and 30 mA cm<sup>-2</sup>. Current density, GNS concentration and surfactants concentration are significantly affected by electrodeposition process. The optimum thickness of Ni-GNS nanocomposite coatings were increased in existence of 0.2 g L<sup>-1</sup> and cationic surfactants (400 ppm S<sub>1</sub> or 300 ppm S<sub>2</sub>). The existence of GNS in Ni-GNS nanocomposite coatings has been authenticated with SEM and EDX analysis.

The highest hardness value was recorded as 509 Hv for the composite coating of Ni-GNS/with S1 compared with 495 Hv for Ni-GNS/with S2 for the other nano composite coatings, pure Ni coatings with and without GNS.

The lowest C.R. was obtained at optimum condition c.d 30 mA cm<sup>-2</sup>, GNS 0.2 g L<sup>-1</sup>, S1 400 ppm and S2 300 ppm in 0.6 M NaCl.

### References

1. Awasthi, S., et al., Interfacial mechanics of carbonaceous reinforcements in electrophoretically deposited nickel coatings. *Surface and Coatings Technology*, **310**, 79-86 (2017).
2. Kolonits, T., et al., Characterization of defect structure in electrodeposited nanocrystalline Ni films. *Journal of The Electrochemical Society*, **163**(3), D107-D114 (2016).
3. Gül, H., et al., Characteristics of electro-co-deposited Ni-Al<sub>2</sub>O<sub>3</sub> nano-particle reinforced metal matrix composite (MMC) coatings. *Wear*, **267**(5), 976-990 (2009).
4. Aruna, S., Lashmi P., and Seema H., The effect of additives on the properties of electrodeposited Ni-zircon composite coatings. *RSC Advances*, **6**(14), 11185-11192 (2016).
5. Abdel Hamid, Z. and Omar A., The relation between anionic/non-ionic surfactant and electrodeposition of nickel-polytetrafluoro ethylene polymer composite. *Anti-Corrosion Methods and Materials*, **46**(3), p. 212-216 (1999).
6. Corrosion Study of Glaze-Ceramics Doped Cement-Kiln-Dust Soaked in Concentrated HCl. *Egypt. J. Chem.* **62**, No. 2 (2019)

- Egyptian Journal of Chemistry*, **53**(1), 117-135 (2010).
7. Gezerman, A.O. and Corbacioglu B.D., Analysis of the characteristics of nickel-plating baths. *International Journal of Chemistry*, **2**(2), 124 (2010).
  8. Ke, Q. and Wang J., Graphene-based materials for supercapacitor electrodes—A review. *Journal of Materiomics*, **2**(1), 37-54 (2016).
  9. Hu, J., et al., A Review on the use of Graphene as a Protective Coating against Corrosion. *Ann J Materials Sci Eng*, **1**(3-2014), (2014).
  10. Ren, Z., et al., Mechanical properties of nickel-graphene composites synthesized by electrochemical deposition. *Nanotechnology*, **26**(6), 065706 (2015).
  11. Khalil, M., et al., Electrodeposition of Ni–GNS–TiO<sub>2</sub> nanocomposite coatings as anticorrosion film for mild steel in neutral environment. *Surface and Coatings Technology*, **275**, 98-111 (2015).
  12. Jabbar, A., et al., Electrochemical deposition of nickel graphene composite coatings: effect of deposition temperature on its surface morphology and corrosion resistance. *RSC Advances*, **7**(49), 31100-31109 (2017).
  13. Potts, J.R., et al., Graphene-based polymer nanocomposites. *Polymer*, **52**(1), 5-25 (2011).
  14. Schuh, B., et al., Mechanical properties, microstructure and thermal stability of a nanocrystalline CoCrFeMnNi high-entropy alloy after severe plastic deformation. *Acta Materialia*, **96**, 258-268 (2015).
  15. Gul, H., et al., A reciprocating wear study on the effect of surfactant concentration and sliding speed in the electro codeposited Ni/SiCp metal matrix composites. *Journal of Composite Materials*, **50**(19), 2603-2616 (2016).
  16. Shrestha, N.K., Miwa I., and Saji T., Composite plating of Ni/SiC using a cationic surfactant with an azobenzene group. *Journal of the Electrochemical Society*, **148**(2), C106-C109 (2001).
  17. Jiang, S., et al., Electrodeposition of Ni-Al 2 O 3 composite coatings with combined addition of SDS and HPB surfactants. *Surface and Coatings Technology*, **286**, 197-205 (2016).
  18. Zaky, M.F., Negm N.A., and Hendawy M., Biocidal activity and corrosion inhibition of some cationic surfactants derived from Thiol polyurethane. *Egyptian Journal of Chemistry*, **61**(1), 45-60 (2018).
  19. Novel Cationic Schiff Base Surfactants: Surface Studies and Biocidal Activities against Bacteria Fungi and Sulfate Reducing Bacteria. *Egyptian Journal of Chemistry*, **55**(2), 201-211 (2012).
  20. Synthesis, Characterization and Thermal Behavior of Novel Acrylate Polymers Based on N-(benzothiazole-2-yl) Maleimide. *Egyptian Journal of Chemistry*, **56**(4), 307-323 (2013).
  21. Hummers Jr, W.S. and Offeman R.E., *Preparation of graphitic oxide*. *Journal of the American Chemical Society*, **80**(6), 1339-1339 (1958).
  22. Wang, D., et al., Preparation, characterization, and electrocatalytic performance of graphene-methylene blue thin films. *Nano Research*, **4**(1), 124-130 (2011).
  23. Ciszewski, A., et al., Effects of saccharin and quaternary ammonium chlorides on the electrodeposition of nickel from a Watts-type electrolyte. *Surface and Coatings Technology*, **183**(2-3), 127-133 (2004).
  24. Abdel Hamid, Z., El-Etre A., and Fareed M., Performance of Ni–Cu–ZrO<sub>2</sub> nanocomposite coatings fabricated by electrodeposition technique. *Anti-Corrosion Methods and Materials*, **64**(3), 315-325 (2017).
  25. Güler, E.S., Effects of electroplating characteristics on the coating properties, in Electrodeposition of Composite Materials, *InTech*. (2016)
  26. Ameer, M., Fekry A., and Bahr M.M., Effect of Streptococcus mutans on the Corrosion Behavior of Nano-Coating Ni-Cr Dental Alloy. *Int. J. Electrochem. Sci.*, **12**, 9652-9664 (2017).
  27. Ameer, M. and Fekry A., Corrosion inhibition of mild steel by natural product compound. *Progress in Organic Coatings*, 2011. **71**(4): p. 343-349.
  28. Ismail, N., et al., Application of Theophylline Anhydrous as Inhibitor of Acid Corrosion of Aluminum. *Egyptian Journal of Chemistry*, **60**(1):95-107 (2017).
  29. Szeptycka, B., *Kształowanie struktury i właściwości elektrolitycznych nanowarstw kompozytowych Ni-SiC, Ni-PTFE i Ni-SiC-PTFE.*: Instytut Mechaniki Precyzyjnej (2009).
  30. Gül, H., et al., Effect of particle concentration

on the structure and tribological properties of submicron particle SiC reinforced Ni metal matrix composite (MMC) coatings produced by electrodeposition. *Applied Surface Science*, **258**(10), 4260-4267 (2012).

31. Chibowski, S., Grządka E., and Patkowski J., Influence of a type of electrolyte and its ionic

strength on the adsorption and the structure of adsorbed polymer layer in the system: polyacrylic acid/SiO<sub>2</sub>. *Croatica Chemica Acta*, **82**(3), 623-631 (2009).

(Received 6/8/2018;  
accepted 6/9/2018)

### تأثير خوافض التوتر السطحي الكاتيونية على الترسيب الكهربى من الطلاء مركب نيكل / شرائح الجراين النانويه كطبقة على شرائح النحاس

ماجده عبده امير<sup>1</sup>، زينب عبد الحميد<sup>2</sup>، محمد شحاته<sup>3</sup>، بلال مصطفى<sup>4</sup>، امانى محمد فكرى<sup>5</sup>  
<sup>1</sup>ا قسم الكيمياء - كلية العلوم - جامعه القاهره - الجيزه - رقم بريدى : ١٢٦١٣ - مصر.  
<sup>2</sup>ا قسم حماية الاسطح والتحكم بالتآكل - معهد الفلزات - حلوان - القاهره - مصر.

تستخدم صفائح الجرافين النانويه (GNS) والمواد الخافضه للتوتر السطحي الموجبه (S1 & S2) للطلاء الكهربائى لمتراكبات النيكل. لديهم دور كبير في زيادة مقاومة التآكل لهذا الطلاء. يتم استخدام حوض النيكل واط مع إضافة GNS كمواضع تقوية ومواد مختلفة لخفض التوتر السطحي لترسيب الطلاء النانوي المركب-Ni (GNS) وتم فحص النتائج واكتشافها. تستخدم التقنيات الكهروكيميائية لفحص مقاومة التآكل لعينات من الطلاء النانوي المركب في 0.6 M NaCl. تشير النتائج الى أن محتوى GNS المدمج يزداد مع زيادة حجم GNS في حوض الطلاء. تتميز كل الطبقات النانويه المركبة Ni-GNS في وجود مادة خافضه للتوتر السطحي بمقاومة أفضل للتآكل من طلاء النيكل. إن أفضل قيمة مقاومة للتآكل تبلغ حوالي 64 kΩ cm<sup>2</sup> وأعلى قيمة صلابة نسبية تبلغ 509 Hv لقطب طلاء المركب من Ni-GNS / مع S1 تقارن مع بقية أقطاب الطلاء النانويه المركبة أو طلاء نيكل نقي.